

# Competing sorting signals guide endolyn along a novel route to lysosomes in MDCK cells

Gudrun Ihrke<sup>1</sup>, Jennifer R. Bruns<sup>2</sup>,  
J. Paul Luzio and Ora A. Weisz<sup>2</sup>

Department of Clinical Biochemistry and Cambridge Institute for Medical Research, University of Cambridge, Wellcome Trust/MRC Building, Cambridge CB2 2XY, UK and <sup>2</sup>Laboratory of Epithelial Cell Biology, Renal-Electrolyte Division, University of Pittsburgh, Pittsburgh, PA 15261, USA

<sup>1</sup>Corresponding author  
e-mail: gi200@cus.cam.ac.uk

**We have examined the trafficking of the mucin-like protein endolyn in transfected, polarized MDCK cells using biochemical approaches and immunofluorescence microscopy. Although endolyn contains a lysosomal targeting motif of the type YXXΦ and was localized primarily to lysosomes at steady state, significant amounts of newly synthesized endolyn were delivered to the apical cell surface. Antibodies to endolyn, but not lamp-2, were preferentially internalized from the apical plasma membrane and efficiently transported to lysosomes. Analysis of endolyn–CD8 chimeras showed that the luminal domain of endolyn contains apical targeting information that predominates over basolateral information in its cytoplasmic tail. Interestingly, surface polarity of endolyn was independent of *O*-glycosylation processing, but was reversed by disruption of *N*-glycosylation using tunicamycin. At all times, endolyn was soluble in cold Triton X-100, suggesting that apical sorting was independent of sphingolipid rafts. Our data indicate that a strong, *N*-glycan-dependent apical targeting signal in the luminal domain directs endolyn into a novel biosynthetic pathway to lysosomes, which occurs via the apical surface of polarized epithelial cells.**

**Keywords:** apical sorting/glycosylation/lipid rafts/  
polarized epithelial cells/targeting motif

## Introduction

Membrane proteins contain sorting motifs that guide them to their intracellular destination by interaction with the cellular sorting machinery. Best understood are motifs that contain a critical tyrosine residue or a 'dileucine' that are located in the cytoplasmic tails of many membrane proteins (reviewed in Heilker *et al.*, 1999). These targeting signals are recognized by adaptor protein (AP) complexes or related proteins, which are recruited to the *trans*-Golgi network (TGN), the plasma membrane (PM) and endosomes, and mediate incorporation into distinct transport vesicles destined for a certain target compartment. Most of these signals allow efficient AP-2-mediated internalization from the PM via clathrin-coated pits (Owen and Luzio, 2000); however, more specific features are required for

sorting at the TGN or endosomes. The affinity of YXXΦ motifs (Φ being a bulky hydrophobic amino acid) for specific adaptors is partially determined by the nature of the amino acids in positions Y+1 to Y+3 (Ohno *et al.*, 1998; Gough *et al.*, 1999). A glycine preceding the tyrosine (Y–1) is a common feature of lysosomal targeting motifs and is necessary for efficient 'direct' transport from the TGN to an endosomal or prelysosomal compartment, bypassing the cell surface (Harter and Mellman, 1992; Höning and Hunziker, 1995). AP-3 is thought to be one of the sorting adaptors on this route (Odorizzi *et al.*, 1998). However, a variable fraction of lysosomal membrane glycoproteins transits the PM *en route* to lysosomes (the 'indirect' route); the size of this fraction depends on the specific protein and cell type (Nabi *et al.*, 1991; Harter and Mellman, 1992). In polarized epithelial cells, this fraction is usually transported to the basolateral PM since its cytoplasmic tyrosine motifs are also recognized by the basolateral sorting machinery (reviewed in Hunziker and Geuze, 1996).

Much less is known about the sorting of proteins to the apical surface of polarized epithelial cells. Basolateral and apical cargo are sorted into different transport vesicles at the TGN in MDCK cells; however, the identity of apical sorting signals is a matter of continued debate (see Ikonen and Simons, 1998; Brown and London, 1998; Mostov *et al.*, 2000 for reviews). Current models envision the budding of apical vesicles from areas of the TGN that are enriched in glycosphingolipids and cholesterol. These lipids are believed to form membrane microdomains into which apical membrane proteins partition due to certain characteristics, such as the presence of a glycosylphosphatidylinositol (GPI) anchor or specific features of their transmembrane (TM) domains. In addition, both *N*- and *O*-glycans in the luminal domains of GPI-linked or TM proteins have been reported to confer apical targeting (Ikonen and Simons, 1998; Mostov *et al.*, 2000). Finally, cytoplasmic signals have also been implicated in apical targeting (e.g. Chuang and Sung, 1998; Gokay *et al.*, 2001), but there is currently no evidence that these signals interact with AP complexes.

Our earlier studies indicated that endolyn, a mucin-like type I membrane protein, contains characteristics of a lysosomal membrane protein, but also has some features usually associated with apical membrane proteins. The C-terminal YXXΦ motif in the short cytoplasmic tail of this protein is necessary and sufficient for lysosomal targeting of a reporter molecule (CD8), despite the absence of a glycine in the Y–1 position (Ihrke *et al.*, 2000a). However, in polarized hepatic WIF-B cells only a fraction of molecules internalized from the basolateral surface was directed into the endosomal/lysosomal pathway; another fraction was sorted to a subapical compartment (SAC), through which apical membrane proteins

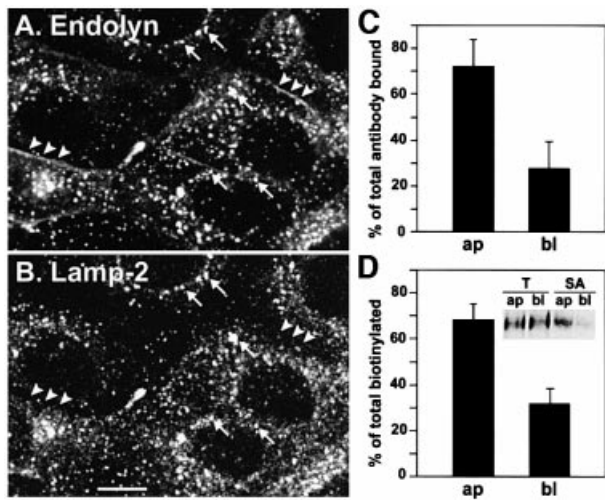


**Fig. 1.** Steady-state localization of endolyn in stably transfected MDCK cells. (A and B) Cells grown on coverslips (non-induced) were fixed, permeabilized, labeled with rabbit anti-endolyn (A) and mouse anti-lamp-2 (B) and processed for indirect immunofluorescence. Arrows point to areas of colocalization; arrowheads denote surface staining of endolyn; bar, 10  $\mu$ m. The merged image is shown in colour as supplementary data at *The EMBO Journal Online*. (C) Binding of [<sup>125</sup>I]anti-endolyn to the apical (ap) or basolateral (bl) cell surface of butyrate-induced cells grown on filters. The percentage of total binding to an apical/basolateral pair of filters (mean  $\pm$  SD of five experiments) is shown. (D) Cell surface biotinylation of induced polarized cells: the apically (ap) or basolaterally (bl) biotinylated fraction of endolyn was recovered from four-fifths of the sample (SA) and expressed as percentage of total calculated from the remaining one-fifth (T). The percentage of total biotinylated endolyn in an apical/basolateral pair of filters (mean  $\pm$  SEM of three experiments performed in duplicate) is plotted; a representative gel is shown in the insert. The average proportion of total endolyn that was biotinylated was 11.8% per filter pair.

move before they reach the apical surface (Ihrke *et al.*, 1998). This finding was puzzling since sorting to lysosomes and to the apical surface is mediated by different mechanisms, which are thought to be mutually exclusive. In the present study, we have therefore attempted to locate apical targeting information in endolyn and to define its significance for the trafficking of this protein in simple polarized epithelial cells, in particular in relation to glycosylation and/or raft-mediated sorting in the biosynthetic pathway. To this end, we have examined the transport routes of endolyn in polarized Madin–Darby canine kidney (MDCK) cells. Our results suggest that, during biosynthetic transport, an *N*-glycan-dependent targeting signal in the luminal domain of endolyn overrides/competes with basolateral and lysosomal sorting information contained in the cytoplasmic tail, causing transport from the TGN to the apical cell surface. This signal does not interfere with efficient lysosomal sorting in apical early endosomes.

## Results

### **Endolyn is localized to lysosomes and the PM of MDCK cells at steady state**

We generated stable MDCK cell lines that express endolyn driven by the butyrate-inducible cytomegalovirus promoter and examined the distribution of endolyn by indirect immunofluorescence. The majority of endolyn

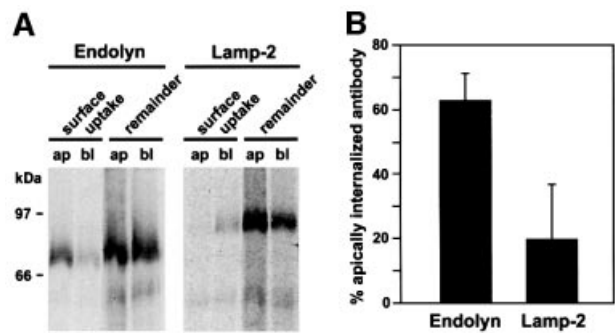


**Fig. 2.** Newly synthesized endolyn is delivered to the apical surface of polarized MDCK cells. Endolyn-expressing cells were radiolabeled for 15 min and chased for 1 h in the presence of mAb to endolyn or lamp-2 added apically (ap) or basolaterally (bl). Antibody–antigen complexes were recovered from cell lysates (surface uptake), followed by immunoprecipitation of remaining antigen. A representative experiment is shown in (A). (B) Apical internalization of mAb expressed as a percentage of total uptake per filter pair [mean  $\pm$  SD of four (endolyn) and five (lamp-2) experiments].

colocalized with lamp-2, indicating its presence in lysosomes (Figure 1A and B, showing non-polarized cells). In addition, some endolyn was detected at the PM, particularly at the apical domain of filter-grown, polarized cells. To quantify the polarized surface distribution, we measured the binding of radioiodinated antibody to endolyn (Figure 1C) and found that  $\sim$ 70% of total surface endolyn was at the apical PM. Domain selective biotinylation gave similar results (Figure 1D).

### **A significant fraction of newly synthesized endolyn is sorted directly from the TGN to the apical surface**

Apical polarity of endolyn could be due to polarized sorting of newly synthesized protein at the TGN or to redistribution after delivery to the cell surface. To distinguish between these possibilities, we radiolabeled endolyn-expressing cells for 15 min and chased in the presence of apically or basolaterally added anti-endolyn monoclonal antibody (mAb). Antibody–antigen complexes collected from the cell lysates should contain any endolyn that transited the apical or basolateral PM during the chase period. Addition of anti-endolyn to the apical chamber resulted in a significantly higher recovery of labeled (newly synthesized) endolyn compared with basolateral addition (Figure 2). As a control, we incubated parallel filters with antibody to lamp-2. Consistent with previous observations (Nabi *et al.*, 1991), this antibody captured little newly synthesized lamp-2 at the apical surface. Therefore, it is unlikely that we saturated any sorting mechanism operating at the TGN by overexpression of endolyn. Our results thus indicate that, in contrast to other lysosomal membrane proteins, a significant fraction of endolyn is sorted apically at the TGN.

### **Endolyn is efficiently internalized from the apical surface and targeted to lysosomes**

To confirm that surface localization of endolyn was transient, we next quantified the rate and extent of uptake of radioiodinated anti-endolyn added to the apical or basolateral chamber (Figure 3). The ratio of apically to basolaterally internalized antibody paralleled endolyn's steady-state distribution, i.e.  $\sim$ 70% of total antibody

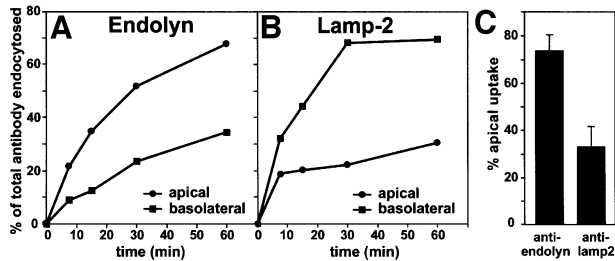


**Fig. 3.** Antibody to endolyn is internalized preferentially from the apical cell surface of polarized MDCK cells. Endolyn-expressing cells were incubated with apically or basolaterally added [ $^{125}$ I]mAb to endolyn (A) or lamp-2 (B) for the times indicated. In (A) and (B), the amount of endocytosed antibody was counted and expressed as a percentage of the total internalized in each filter pair at 60 min. (C) Apical uptake after 60 min [mean  $\pm$  SD from nine (endolyn) and eight (lamp-2) experiments].

uptake occurred from the apical side. By contrast, anti-lamp-2 was preferentially endocytosed from the basolateral PM of polarized cells, as expected (Nabi *et al.*, 1991).

Internalized antibody could be recycled, delivered to lysosomes (where it would be rapidly degraded) or transcytosed to the opposite cell surface. To determine whether it reached lysosomes, we followed the fate of [ $^{125}$ I]mAb endocytosed from the apical or basolateral surface (Figure 4). When internalized from the apical surface, ~40% of the radioactivity was trichloroacetic acid (TCA) soluble after a 1 h pulse and 2 h chase period, consistent with efficient delivery of antibody to lysosomes. It is unlikely that the degraded fraction represents dissociated antibody because delivery of apically internalized fluid phase markers to lysosomes in MDCK cells is poor (<10%; Bomsel *et al.*, 1989). Approximately 27% of the antibody was recycled, while transcytosis to the opposite chamber was insignificant (<10%). Basolaterally internalized antibody was less efficiently degraded and remained instead in non-degradative intracellular compartments, consistent with prolonged trafficking through endosomal compartments as seen in WIF-B cells (Ihrke *et al.*, 1998).

Lysosomal delivery of endolyn internalized from the apical surface was verified by indirect immunofluorescence. Cells were incubated with apically added anti-endolyn mAb for 10 min and chased for various periods before fixation and colabeling with endocytic markers. At the earliest time point studied, i.e. 10 min uptake with no chase, there was almost exclusive colocalization of internalized antibody with the early endosomal antigen 1 (EEA1) in structures located between the nucleus and the apical surface (Figure 5A and B). These structures were mostly identical to those containing fluid phase marker (FITC-dextran) internalized from the apical surface over the same period of time (not shown). Some EEA1-positive, but mAb-negative structures were found in more basal regions. When the cells were chased from 10 to 120 min, there was increasingly less overlap of internalized anti-endolyn with early endosomal markers and more overlap with steady-state endolyn, indicative of arrival in late endosomal/lysosomal compartments (Figure 5C and D, compare with Figure 1). At intermediate time points, we detected minor overlap with transferrin

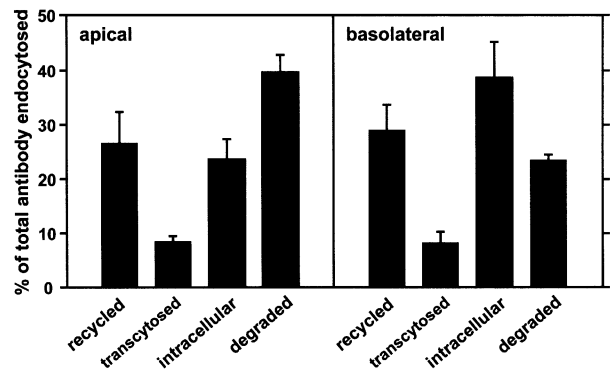


**Fig. 4.** Fate of internalized anti-endolyn. Polarized MDCK cells expressing endolyn were incubated with apically or basolaterally added [ $^{125}$ I]anti-endolyn for 1 h at 37°C, surface-stripped and incubated without antibody for 2 h. Recycled, transcytosed, intracellular (intact) and degraded antibody fractions were calculated as described in Materials and methods (mean  $\pm$  SEM of six apical and eight basolateral uptake experiments performed in triplicate).

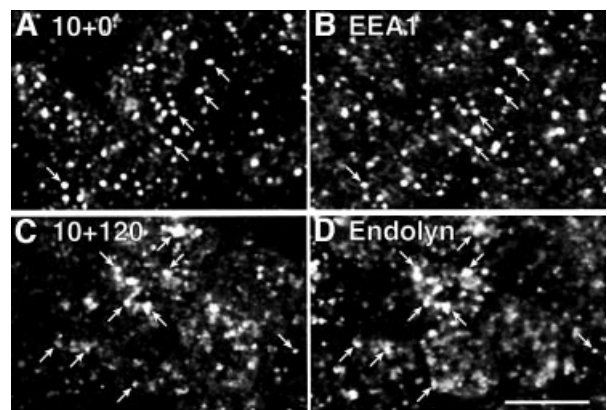


**Fig. 5.** Apically internalized endolyn is delivered to lysosomes. Polarized MDCK cells expressing endolyn were incubated with apically added anti-endolyn mAb for 10 min, washed and incubated without antibody for 0 min (A and B) or 120 min (C and D). After fixation, cells were double-labeled with rabbit antibodies to EEA-1 (B) or endolyn (D), followed by incubation with Cy3 anti-mouse and FITC-anti-rabbit antibodies, and analyzed by confocal microscopy. Arrows point to structures that contain both endocytosed mAb and the respective marker; bar, 10  $\mu$ m.

endocytosed from the basolateral surface, marking the common recycling compartment, and with rab11, which is enriched in apical recycling endosomes (not shown). Altogether these results are in good agreement with our biochemical data, showing that the bulk of endolyn is efficiently endocytosed from the apical PM and transported from early sorting endosomes to lysosomes.

#### **The luminal domain of endolyn contains dominant apical sorting information**

Apical sorting of newly synthesized endolyn in MDCK cells is consistent with our previous finding in polarized WIF-B cells that basolaterally endocytosed endolyn is directed into the transcytotic pathway to a SAC (Ihrke *et al.*, 1998). There are two possible explanations for these observations: either the tyrosine motif in the cytoplasmic tail of endolyn does not function as a basolateral signal or dominant apical targeting information in other domains of the protein can override the basolateral cytoplasmic motif. We tested these possibilities using chimeras in which both

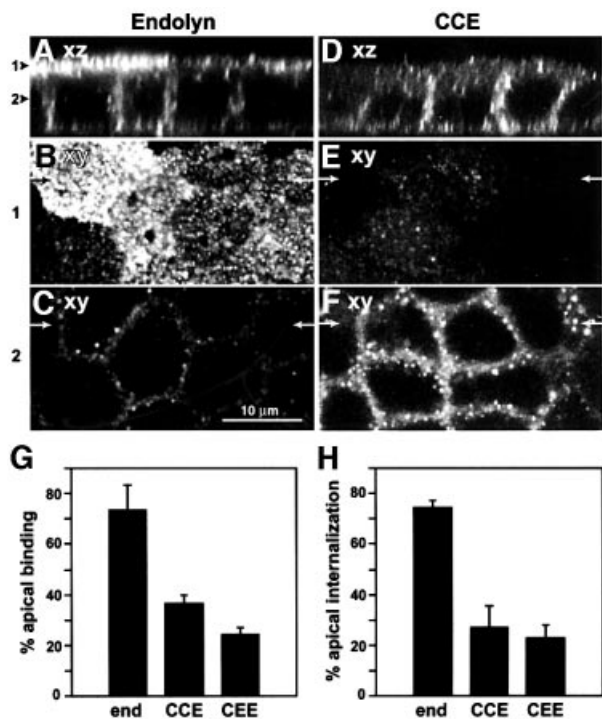


**Fig. 6.** Basolateral polarity of CCE and CEE chimeras. (A–F) Filter-grown MDCK cells expressing endolyn (A–C) or CCE (D–F) were incubated for 5 min at 37°C with anti-endolyn or anti-CD8 mAb, respectively, added to both chambers. After fixation, cells were incubated with Cy3 anti-mouse (A–C) or Texas Red anti-rat antibodies (D–F) and further processed for confocal microscopy. Side views (xz) are shown in (A) and (D), arrowheads indicate the positions of the xy sections depicted in (B) and (E) (1, apical surface) and (C) and (F) (2, middle section of the cells). Arrows in (B), (C), (E) and (F) mark the positions of the xz-sections. (G and H) Quantitative comparison of [<sup>125</sup>I]mAb binding and uptake in cells expressing endolyn (end), CCE or CEE. Cells were incubated with apically or basolaterally added [<sup>125</sup>I]mAb to endolyn or CD8 for 60 min at 0°C (G) or 37°C (H). Apically bound (G) or internalized (H) antibody was expressed as a percentage of total in an apical/basolateral filter pair (average ± range of two experiments performed in duplicate).

the luminal and TM domains of endolyn (CCE), or only its luminal domain (CEE), were replaced with that of CD8 (an *O*-glycosylated type I plasma membrane protein). To visualize the fraction of CD8 chimeras transiting the apical or basolateral cell surface, polarized, stably transfected cells were incubated for 5 min with anti-CD8 mAb added to both sides of the same filter. Little antibody was seen at or close to the apical surface, but basolaterally bound and internalized antibody was detected in both cell lines (CCE shown in Figure 6D–F). In control cells expressing endolyn, anti-endolyn was predominantly seen at or below the apical PM (Figure 6A–C), consistent with our biochemical experiments (see Figure 3). These observations were confirmed in quantitative experiments using [<sup>125</sup>I]mAbs. For both chimeras, binding and endocytosis of anti-CD8 occurred preferentially from the basolateral cell surface (Figure 6G and H, respectively). In comparison, MDCK cells stably expressing wild-type CD8 bound antibody primarily at the apical cell surface [ $77.4 \pm 8.4\%$  ( $\pm$ SD);  $n = 4$ ], confirming an earlier study (Migliaccio *et al.*, 1990), and no antibody was internalized after 60 min at 37°C (not shown). We also examined the polarized delivery of newly synthesized CCE and CEE by

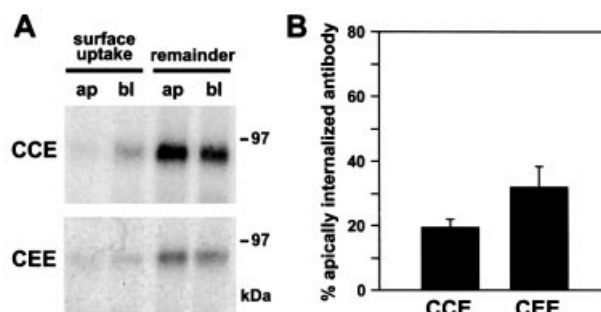


**Fig. 7.** Newly synthesized CCE and CEE are delivered primarily to the basolateral cell surface. Polarized MDCK cells expressing CCE or CEE were radiolabeled for 15 min and chased for 90 min in the presence of leupeptin and anti-CD8 mAb added apically (ap) or basolaterally (bl). Uptake was quantified as described in Figure 2. (A) Representative autoradiogram; (B) mean apical uptake ± SD of four determinations.

antibody capture (Figure 7). As expected, the majority of newly synthesized molecules reaching the cell surface traversed the basolateral PM *en route* to lysosomes. These results show that the cytoplasmic tail of endolyn contains basolateral targeting information capable of redirecting the CD8 reporter to lysosomes via the basolateral surface. They also indicate that the TM domain of endolyn does not contain apical targeting information that overrides the basolateral sorting signal. Thus, dominant apical targeting information is likely to be present in the luminal domain of endolyn.

To confirm this conclusion, we generated the construct ECCΔ consisting of the luminal domain of endolyn linked to the TM domain and the first 10 amino acids of the cytoplasmic tail of CD8. We chose to delete most of CD8's cytoplasmic domain so that it would be sufficient to anchor the construct in the membrane but most likely not contribute any targeting information. We also constructed a mutant version of endolyn (EEE<sub>Y-A</sub>) in which the tyrosine in the cytoplasmic tail was substituted by an alanine. This tail should be neutral, i.e. not be able to confer basolateral or lysosomal targeting. When examined by indirect immunofluorescence, ECCΔ and EEE<sub>Y-A</sub> were both localized primarily at the apical PM at steady state (Figure 8A and B). We determined by cell surface biotinylation (Figure 8C) and binding of [<sup>125</sup>I]anti-endolyn at 0°C (not shown) that ~70% of ECCΔ and 80% of EEE<sub>Y-A</sub> (of total surface antigen) were apical. Finally, to examine whether apical sorting information in the luminal domain of endolyn was recognized independently of membrane association of the protein, we created a soluble construct lacking the TM and cytoplasmic domains (En<sub>sol</sub>). About 80% of En<sub>sol</sub> was secreted into the apical medium (Figure 8D). Taken together, these results indicate that independent targeting information present in endolyn's luminal domain is dominant over the tyrosine-containing motif in the cytoplasmic domain and diverts molecules from the direct lysosomal and basolateral routes into a pathway leading to the apical cell surface.

#### **Apical transport of endolyn is N-glycan dependent and does not correlate with detergent insolubility**

Since endolyn is a highly glycosylated protein, we sought to investigate whether *O*-glycans or *N*-glycans were involved in its apical sorting. Incubation of MDCK cells

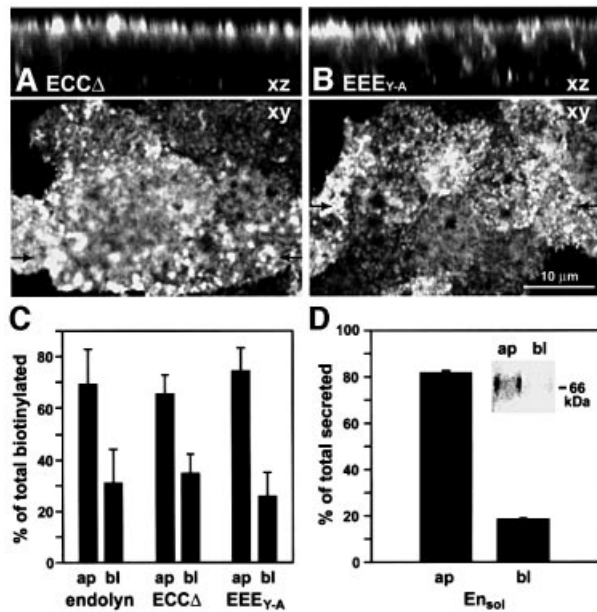


**Fig. 8.** Apical polarity of  $ECC\Delta$ ,  $EEE_{Y-A}$  and  $En_{sol}$  in stably transfected MDCK cells. (**A** and **B**) Steady-state distribution of  $ECC\Delta$  and  $EEE_{Y-A}$  revealed by confocal microscopy. Upper panels show side views (xz) of cells at the positions indicated by arrows in the lower panels, which depict xy views of the apical surface. (**C**) Surface biotinylation of cells expressing endolyn,  $ECC\Delta$  or  $EEE_{Y-A}$ . Biotinylation fractions were determined as described in Figure 1 (mean  $\pm$  SD from four experiments). (**D**) Cells expressing  $En_{sol}$  were metabolically labeled for 4 h and secreted  $En_{sol}$  was immuno-precipitated from the medium. The average percent apical and basolateral secretion of total ( $\pm$  range) from two experiments is plotted; a representative sample pair is shown inset.

expressing wild-type endolyn with 4 mM benzyl-*N*-acetyl- $\alpha$ -D-galactosaminide (benzyl-GalNAc), which disrupts *O*-glycosylation beyond the addition of GalNAc, resulted in reduced mobility of endolyn by SDS-PAGE (Figure 9A). This anomalous shift is typical for undersialylated mucin-like proteins (see e.g. Altschuler *et al.*, 2000). However, impaired *O*-glycosylation had no effect on the steady-state distribution of endolyn (Figure 9B). In contrast, blocking *N*-glycosylation with tunicamycin resulted in a redistribution of cell surface endolyn from predominantly apical to mostly basolateral (Figure 9C and D). This was particularly obvious in experiments in which *N*-glycosylation was not completely inhibited and the distribution of biotinylated endolyn with or without N-linked sugars could be compared in the same lanes (Figure 9C). Moreover, newly synthesized non-*N*-glycosylated endolyn was preferentially directed to the basolateral PM, suggesting that the new steady-state distribution was due to altered sorting in the TGN (not shown). Importantly, overall transport to the cell surface was not markedly impaired, as the ratio of surface to total endolyn remained largely unchanged after both drug treatments.

Another typical feature of apical membrane proteins is inclusion in glycolipid rafts, which sometimes depends on the presence of glycans (Alfalah *et al.*, 1999). Thus, we examined whether endolyn was associated with detergent-insoluble microdomains. Cells coexpressing endolyn and virally introduced influenza hemagglutinin (HA) were radiolabeled and solubilized in ice-cold Triton

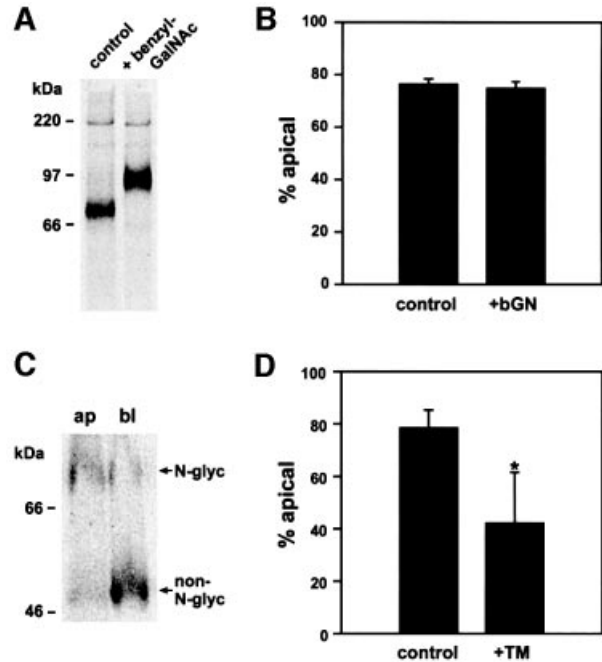


**Fig. 9.** Apical delivery of endolyn is independent of *O*-glycosylation, but dependent on *N*-glycosylation. (**A**) Endolyn-expressing MDCK cells were incubated with or without 4 mM benzyl-GalNAc (bGN) for 2 h and radiolabeled for 30 min ( $\pm$  drug). (**B**) Cells were drug-treated as above and steady-state binding of [ $^{125}$ I]anti-endolyn was assessed as described in Figure 1C (mean  $\pm$  range from two experiments). (**C** and **D**) Cells were radiolabeled for 3 h in the presence of 2  $\mu$ g/ml tunicamycin (TM), chased for 1 h and then biotinylated at the apical or basolateral PM. In the example shown in (C), tunicamycin did not completely inhibit *N*-glycosylation, so that the reversed polarities of *N*-glycosylated and non-*N*-glycosylated endolyn are readily apparent (79.7% glycosylated and 30.6% non-*N*-glycosylated endolyn at the apical PM). (**D**) Mean percentages of *N*-glycosylated (control) and non-*N*-glycosylated endolyn (tunicamycin-treated cells) at the apical surface ( $\pm$  SD of five experiments).

X-100 (TX-100). Both endolyn and lamp-2 were mostly soluble, independently of the pulse-chase times, whereas a considerable fraction of HA was insoluble, as described previously (Scheiffele *et al.*, 1997) (Figure 10A). Recently, evidence has emerged for the existence of separate lipid microdomains in the TGN that are insoluble in Lubrol WX (Röper *et al.*, 2000). Therefore, we tested whether endolyn was insoluble in the Lubrol-like non-ionic detergent polyoxyethylene ether W1 (PE W1). Interestingly, a significant fraction of endolyn was found to be transiently (after a 1 h pulse with no chase) insoluble in this non-ionic detergent; however, lamp-2 behaved similarly, suggesting that this characteristic was not related to apical trafficking of endolyn (not shown). Moreover, disruption of glycolipid rafts by treatment with fumonisin B<sub>1</sub> had no effect on the polarized distribution of endolyn as measured by [ $^{125}$ I]anti-endolyn binding (not shown). Together these data indicate that apical sorting of endolyn occurs by a mechanism that depends on the presence of *N*-glycans, but does not appear to involve segregation into glycolipid rafts.

## Discussion

Lysosomal membrane proteins use a combination of direct and indirect pathways via the cell surface to reach

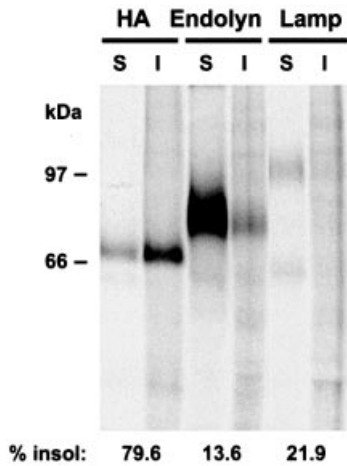


**Fig. 10.** Endolyn is soluble in cold TX-100. MDCK cells expressing endolyn and HA were radiolabeled for 1 h, chased for 1 h and solubilized in ice cold TX-100. Detergent-soluble (S) and -insoluble (I) fractions of HA, endolyn and lamp-2 were quantified as described in Materials and methods. Similar results were obtained in at least three determinations.

lysosomes. Typically, proteins traversing the indirect (often the minor) pathway are directed to the basolateral surface of polarized epithelial cells due to the presence of a targeting motif in their cytoplasmic tails (Hunziker and Geuze, 1996). Here we show that another lysosomal pathway exists that involves transit through the apical PM of MDCK cells. This pathway is used to a significant extent by endolyn, a type I membrane protein with a C-terminal tyrosine motif similar to some other lamps, which on its own confers lysosomal and basolateral sorting. Apical targeting along the biosynthetic pathway was conferred by dominant sorting information located in the luminal domain of endolyn, was *N*-glycan dependent and appeared to occur via a raft-independent mechanism.

#### **A significant fraction of endolyn traffics via the apical cell surface**

The extent of lysosomal delivery of membrane proteins via the direct pathway varies depending on the specific protein and cell type, but is generally facilitated by a GYXXΦ motif positioned at the C-terminus of a short cytoplasmic tail (Hunziker and Geuze, 1996). The YHTL motif of endolyn meets the second criterion, but is not preceded by a glycine and binds with significantly lower affinity to the μ-subunit of AP-3 compared with the tyrosine motif of lamp-1 in the yeast two-hybrid system (Ihrke *et al.*, 2000a,b). This seems to correlate with a more prominent use of the indirect pathway to lysosomes in MDCK cells. Compared with lamp-2, the relative amount of endolyn detected at the PM at steady state was higher, consistent with earlier studies (Croze *et al.*, 1989; Ihrke *et al.*, 1998). Moreover, a significant fraction (up to ~50%) of newly synthesized endolyn became accessible to antibody added to the medium. Importantly, ~70% of this fraction was captured at the apical surface and a similar apical to basolateral ratio was seen at steady state, setting endolyn apart, in this respect, from all other lysosomal membrane proteins that have been studied.

#### **Apical sorting of endolyn is dominant over basolateral sorting at the TGN**

The cytoplasmic tail of endolyn contains basolateral targeting information strong enough to redirect the luminal domain of CD8 to the basolateral surface, even though full-length CD8 is preferentially targeted to the apical PM (Migliaccio *et al.*, 1990; this study). Thus, it is unlikely that apical targeting of endolyn occurs by default. Since both reporter constructs with the CD8 luminal domain (CCE and CEE) were targeted basolaterally, the TM domain of endolyn does not appear to be essential for apical sorting. Membrane-associated constructs that contained endolyn's luminal domain and either the presumed neutral TM and cytoplasmic domains of CD8 (ECCΔ) or an inactivated tyrosine motif (EEE<sub>Y-A</sub>) were targeted with apical polarity similar to that of wild-type endolyn. Moreover, a soluble endolyn construct was secreted primarily apically. This indicates that dominant sorting information in the luminal domain directs endolyn to the apical surface, successfully competing with tyrosine motif-mediated sorting into basolateral and direct lysosomal pathways. To our knowledge this is the first case of a wild-type protein where this has been observed, and confirms an earlier study using chimeric proteins (Jacob *et al.*, 1999). Some basolaterally directed proteins, including lamp-1, contain recessive apical sorting information that directs protein localization only upon deletion or inactivation of the basolateral targeting motifs (Hunziker *et al.*, 1991). Also, introduction of cytoplasmic tyrosine motifs in some apical membrane proteins causes their redirection to the basolateral surface (e.g. Brewer and Roth, 1991), adding to the examples of tyrosine motifs dominating over apical targeting information. However, contrary to previous suggestions (Gut *et al.*, 1998; Ikonen and Simons, 1998; Mostov *et al.*, 2000) our results are more consistent with the view that there is no strict hierarchy of basolateral and apical sorting signals.

#### ***N*-glycans play a role in sorting of endolyn to the apical surface**

*N*-glycans could facilitate apical sorting by several mechanisms (reviewed in Rodriguez-Boulan and Gonzalez, 1999). The reversed polarity of endolyn during surface delivery and at steady state caused by blocking *N*-linked glycosylation is consistent with a model by which apical sorting occurs via the specific recognition of apical cargo by an *N*-glycan receptor (Scheiffele *et al.*, 1995). Alternatively, glycans could affect the conformation of a protein, exposing a proteinaceous signal and/or promoting association with membrane microdomains that give rise to apical transport vesicles. However, the dominance of endolyn's apical targeting signal over the cytoplasmic tyrosine motif argues for a high-affinity sorting mechanism. Importantly, we could not find evidence for raft-mediated sorting of endolyn (see below). Non-*N*-glycosylated endolyn in tunicamycin-treated cells was efficiently transported to the cell surface, suggesting that endolyn was properly folded and readily exported from the endoplasmic reticulum. However, it is possible that *N*-glycans are not the only determinant of the apical targeting signal or contribute indirectly to its formation. There are eight potential *N*-glycosylation sites in endolyn, two in the N-terminal mucin-like domain, four

in the postulated globular middle region of the luminal domain and two between this region and the TM domain (Ihrke *et al.*, 2000a). Which of these sites are important for apical sorting remains to be established. Endolyn is one of the first examples of a naturally occurring membrane protein making use of *N*-glycans as an apical sorting determinant, strengthening the view that this mechanism is of physiological importance (Scheiffele *et al.*, 1995; Benting *et al.*, 1999).

We were surprised that *O*-glycosylation did not appear to play a role in apical sorting of endolyn. Unlike lamp-2, which is more highly *N*-glycosylated than *O*-glycosylated, the majority of oligosaccharides on endolyn are O-linked. These glycans are concentrated in the N-terminal and C-terminal regions of the luminal domain. *O*-glycan-rich regions have been implicated previously in apical sorting of the neurotrophin receptor and various intestinal brush border enzymes (Yeaman *et al.*, 1997; Alfalah *et al.*, 1999; Zheng *et al.*, 1999). Terminal sialic acids appear to be crucial for correct sorting of at least some apical membrane proteins (Huet *et al.*, 1998; Ulloa *et al.*, 2000). However, although benzyl-GalNAc treatment significantly reduced sialylation of endolyn, its polarized sorting was unaffected.

#### **Apical sorting of endolyn appears to be independent of association with rafts**

Insolubility in cold TX-100 is a hallmark of various apical membrane proteins, including sucrase–isomaltase, a TM protein (Garcia *et al.*, 1993; Alfalah *et al.*, 1999). It is generally accepted that detergent insolubility is a good indicator of the affinity of proteins for glycolipid rafts, although the relationship between rafts and apical transport vesicles is not understood (Brown and London, 1998). As endolyn was soluble in cold TX-100, by this measure, sorting of endolyn does not occur via lipid rafts. Moreover, treatment with fumonisin B1, an inhibitor of sphingolipid synthesis, which has been shown to impair apical sorting in other cases (Alfalah *et al.*, 1999; Lipardi *et al.*, 2000), did not affect the trafficking of endolyn. While apical sorting of GPI-linked proteins generally involves association with sphingolipid rafts, this seems to apply only to some TM proteins (Scheiffele *et al.*, 1997; Alfalah *et al.*, 1999). In fact, other known TM proteins that rely on *N*-glycans for apical sorting do not appear to partition into rafts (Benting *et al.*, 1999; Martínez-Maza *et al.*, 2001). Since not all apically targeted proteins are TX-100 insoluble in the biosynthetic pathway, at least two mechanisms must exist by which these proteins are sorted into apical transport vesicles (Arreaza and Brown, 1995; Alonso *et al.*, 1997; Zheng *et al.*, 1999; Lipardi *et al.*, 2000). Whether this correlates with different classes of vesicle and independent pathways from the TGN to the apical PM or reflects subdomains of one type of vesicle is currently unclear.

#### **Sorting preferences may differ in the TGN and in apical endosomes**

Our biochemical and immunofluorescence data indicate that internalized anti-endolyn antibodies are delivered predominantly to lysosomes via EEA1-positive endosomes. Since endolyn is apparently able to interact not only with AP complexes but also with apical sorting

machinery, at least three pathways compete for recruitment of endolyn both in the TGN and in endosomes: the (direct) lysosomal, the basolateral and the apical delivery routes. Our results are compatible with two scenarios. In the first, endolyn sorting to lysosomes could occur via an iterative process, whereby a similar proportion of endolyn is diverted to lysosomes from the TGN and from endosomes (following apical delivery and internalization). Alternatively, apical sorting could be less and lysosomal sorting more efficient from apical endosomes than from the TGN, such that the majority of endolyn is directed to lysosomes once it is internalized from the apical surface. Our finding that recycling from apical endosomes was less pronounced compared with lysosomal transport speaks in favor of the second model.

In summary, our results show that endolyn follows a complex intracellular route as a result of two targeting motifs that compete with one other at various sorting stations. In contrast to proteins that contain multiple sorting motifs in their cytoplasmic tails, such as the polymeric IgA receptor and the transferrin receptor (Aroeti and Mostov, 1994; Odorizzi and Trowbridge, 1997), endolyn makes use of a cytoplasmic sorting motif in combination with sorting information contained in its luminal domain. This results in a pathway, so far unique, that leads to lysosomal delivery via the apical cell surface. Studies of the human ortholog of endolyn (CD164) indicate that the surface pool of this protein is involved in cell–cell interaction and regulation of cell proliferation in hematopoietic stem cells (Zannettino *et al.*, 1998). Moreover, the relative amount of CD164 at the cell surface and in recycling endosomes compared with the lysosomal pool seems to be regulated (Chan *et al.*, 2001). Thus, trafficking via the cell surface appears to be an intrinsic property of endolyn and to relate to its function. The role of endolyn at the apical cell surface of polarized epithelial cells is currently unclear; however, its unusual trafficking route might be of functional importance.

## **Materials and methods**

### **Antibodies and reagents**

The mouse mAbs to rat endolyn (501 and 502) have been described (Ihrke *et al.*, 1998); both antibodies were used interchangeably with similar results. A rabbit antiserum (No. 6431) against the luminal domain of rat endolyn expressed as a glutathione-*S*-transferase (GST) fusion protein was prepared by Murex (Cambridge, UK). The mouse mAb to canine lamp-2 (AC17) was a gift from E.Rodríguez-Boulán (Cornell University, New York) (Nabi *et al.*, 1991). The rat mAb to the  $\alpha$ -chain of human CD8 (Campath 8c) was kindly provided by G.Hale (Oxford University, UK) and rabbit antiserum against human EEA1 (No. 243) by M.J.Clague (University of Liverpool, UK) (Bindon *et al.*, 1989; Mills *et al.*, 1998). The rabbit antibody to rab11 was from Zymed. Texas Red anti-rat was from Molecular Probes, other secondary antibodies were from Jackson ImmunoResearch. Tunicamycin, benzyl-GalNAc and PE W1 were from Sigma.

### **cDNA constructs**

The cDNA of wild-type rat endolyn, human CD8  $\alpha$ -chain cDNA and a chimeric construct of the luminal and TM domains of CD8 joined to the cytoplasmic tail of endolyn (CCE) have been described (Ihrke *et al.*, 2000a). These cDNAs and the constructs described below were subcloned behind the butyrate-inducible cytomegalovirus promoter of the pCB6 vector (Brewer and Roth, 1991) and verified by DNA sequencing. To construct the CEE chimera, the TM and cytoplasmic tail domains of endolyn were amplified by PCR, creating an *EcoRV* site at the 5'-end, and joined with luminal domain of CD8. The resulting amino acid sequence

expressed at the luminal/TM domain boundary was DFACDIASFI. To obtain the EEE<sub>Y-A</sub> construct, a tyrosine to alanine mutation in the cytoplasmic tail motif of endolyn was introduced by PCR. To generate the ECCΔ chimera, we first constructed a chimera ECC containing the luminal domain of endolyn (amplified by PCR) and the TM and cytoplasmic tail domains of CD8, and then deleted 19 amino acids at the C-terminus, also by PCR. The amino acid sequence expressed at the luminal/TM domain boundary after joining of the fragments (*EcoRV*) was KSTFDIYIWA. The ECCΔ construct ended with the amino acids KRLKRRRVCK. The construct En<sub>sol</sub> consisting of the luminal domain of endolyn was prepared by PCR. Primer sequences will be provided on request.

### Cell culture

Stable transfectants were generated in MDCK II cells as described previously (Weisz *et al.*, 1992) and plated at superconfluence onto Transwells (0.4 μm pore, Costar) 3–5 days before each experiment. For most constructs, at least two individual clones and mixed populations of drug-resistant cells were tested and gave similar results; analysis of EEE<sub>Y-A</sub>, ECCΔ and En<sub>sol</sub> was performed with mixed populations. In most experiments, cells were induced with 2 mM butyrate for 18–21 h before the experiment, which increased expression ~2-fold. Identical results were obtained with uninduced cells.

### Immunofluorescence microscopy

Cells were fixed by adding 4% paraformaldehyde in 100 mM cacodylate buffer (3 mM CaCl<sub>2</sub>, 3 mM MgCl<sub>2</sub>, 3 mM KCl pH 7.5), warming to 37°C and leaving the cells on a shaker for 15 min at room temperature. Cells were permeabilized with 0.1% TX-100/phosphate-buffered saline (PBS) for 10 min, blocked with 1% bovine serum albumin (BSA)/PBS and otherwise treated as described (Chan *et al.*, 2001). Confocal images were collected using a Leica TCS SP system equipped with a 63× Leitz Plan-Apo objective (NA 1.4) at a resolution of 1024 × 1024 pixels and a zoom of 2.0–3.0. Adobe Photoshop software was used for image processing.

For antibody uptake before fixation, cells were incubated with 50 μg/ml mAb to endolyn or 140 μg/ml mAb to CD8 in regular culture medium supplemented with 20 mM HEPES at 37°C. Filters were washed twice in a large volume of HEPES-buffered serum-free medium containing 4 mg/ml BSA before further incubation in regular medium at 37°C (chase), or additionally in PBS before fixation. In time-course experiments, 21 μM leupeptin was included during all incubation steps to prevent antibody degradation in late endocytic compartments.

### Delivery of newly synthesized proteins

The polarized delivery of newly synthesized endolyn, lamp-2, CCE or CEE to the cell surface was assessed as described with minor modifications (Nabi *et al.*, 1991). Briefly, cells were starved for 30 min in cysteine-free medium, radiolabeled for 15 min with [<sup>35</sup>S]cysteine, then chased for 1 h in the presence of apically or basolaterally added mAbs to endolyn (50 μg/ml), lamp-2 (100 μg/ml) or CD8 (50 μg/ml). After washing, the cells were solubilized in 50 mM Tris-HCl, 2% NP-40, 0.4% deoxycholate, 62.5 mM EDTA, 1 μg/ml aprotinin pH 8.0, and antibody-antigen complexes removed by incubation with protein G-Sepharose. Fresh antibody and protein G-Sepharose were added to precipitate remaining unbound antigen. Samples were analyzed by SDS-PAGE, and the percentage of total labeled protein recovered during the first antibody incubation was quantified using a phosphorimager (Personal Molecular Imager FX, Bio-Rad), using Quantity One software.

### Cell surface biotinylation

Cells were starved as above, pulse-labeled for 3 h with 1.6 mCi/ml [<sup>35</sup>S]cysteine, then chased for 1 h. Biotinylation was performed as described in Altschuler *et al.* (2000). After solubilization and immunoprecipitation (see above), samples were eluted with 100 μl 2% SDS–50 mM Tris pH 7.4. Four-fifths of the eluate was incubated overnight with immobilized streptavidin (Pierce) to precipitate biotinylated proteins; the remainder was used to determine the total after SDS-PAGE.

### Surface binding, internalization and fate of [<sup>125</sup>I]antibodies

Monoclonal antibodies to endolyn, lamp-2 and CD8 were iodinated as described (Breitfeld *et al.*, 1989). Pairs of filters were incubated with apically or basolaterally added [<sup>125</sup>I]mAb in MEM/BSA (MEM, 0.6% BSA, 20 mM HEPES pH 7.4) containing 40 μM leupeptin for 1 h at 0°C (surface binding) or 37°C (internalization) and rapidly washed five times with MEM/BSA. To measure surface binding, filters were cut out of their inserts and the amount of [<sup>125</sup>I]mAb in each sample was determined using

a γ counter (Packard Instrument Co.). Percent apical antibody binding was calculated from the total antibody bound to each filter pair. To measure internalization, cells were incubated with 25 μg/ml L-1-tosylamido-2-phenylethyl chloromethyl ketone-treated trypsin to remove residual surface-bound antibody, rinsed, excised and counted. Untransfected MDCK cells were treated identically to determine non-specific antibody binding or uptake, and these values were subtracted from those of transfected cells. Total uptake of anti-endolyn and anti-CD8 by parental cells was ~5% and 20% that of transfectants, respectively. To measure the fate of internalized antibody, leupeptin was omitted during the incubation with [<sup>125</sup>I]mAb (1 h, 37°C). After stripping of the cell surface with trypsin, cells were incubated with 50 μg/ml soybean trypsin inhibitor for 10 min on ice, and then incubated for 2 h at 37°C in MEM/BSA. The apical and basolateral media were collected, the cells were solubilized and all samples were TCA precipitated. Lysosomal delivery of antibody was calculated as the total amount of TCA-soluble counts recovered in cell and media fractions. The amount of antibody recycled was calculated as the percentage of total antibody recovered in the compartment from which it was internalized and transcytosed antibody as the percentage recovered in the opposite compartment.

### Determination of detergent insolubility

MDCK cell lines stably expressing endolyn were coinfecting with replication-defective recombinant adenoviruses encoding HA and the tetracycline transactivator as described (Henkel *et al.*, 1998). After 16–24 h, cells were radiolabeled and chased for the periods indicated and solubilized in ice-cold TNE (250 mM Tris-HCl, 150 mM NaCl, 5 mM EDTA pH 7.5) containing 1% TX-100 for 20 min. After centrifugation at 4°C for 20 min at 16 000 g supernatants and pellets were separated, the latter solubilized and endolyn, lamp-2 or HA were immunoprecipitated, analyzed by SDS-PAGE and quantified as above.

### Supplementary data

Supplementary data for this paper are available at *The EMBO Journal* Online.

## Acknowledgements

We thank Gregory Gibson for technical assistance and Drs Enrique Rodriguez-Boulan, Geoff Hale and Michael Clague for their generous gifts of antibodies. We are indebted to Drs Patrick Sissons and Tony Minson for access to the Leica confocal microscope and to Drs Gerard Apodaca and Rebecca Hughey for helpful comments on the manuscript. This work was supported by grants from The Wellcome Trust (057263) to G.I. and J.P.L., the National Institutes of Health (DK54407) to O.A.W. and by Dialysis Clinic Inc. The Cambridge Institute for Medical Research is in receipt of a strategic award from The Wellcome Trust.

## References

- Alfalah, M., Jacob, R., Preuss, U., Zimmer, K.P., Naim, H. and Naim, H.Y. (1999) O-linked glycans mediate apical sorting of human intestinal sucrose-isomaltase through association with lipid rafts. *Curr. Biol.*, **9**, 593–596.
- Alonso, M.A., Fan, L. and Alarcon, B. (1997) Multiple sorting signals determine apical localization of a nonglycosylated integral membrane protein. *J. Biol. Chem.*, **272**, 30748–30752.
- Altschuler, Y., Kinlough, C.L., Poland, P.A., Bruns, J.B., Apodaca, G., Weisz, O.A. and Hughey, R.P. (2000) Clathrin-mediated endocytosis of MUC1 is modulated by its glycosylation state. *Mol. Biol. Cell.*, **11**, 819–831.
- Aroeti, B. and Mostov, K.E. (1994) Polarized sorting of the polymeric immunoglobulin receptor in the exocytic and endocytic pathways is controlled by the same amino acids. *EMBO J.*, **13**, 2297–2304.
- Arreaza, G. and Brown, D.A. (1995) Sorting and intracellular trafficking of a glycosylphosphatidylinositol-anchored protein and two hybrid transmembrane proteins with the same ectodomain in Madin–Darby canine kidney epithelial cells. *J. Biol. Chem.*, **270**, 23641–23647.
- Benting, J.H., Rietveld, A.G. and Simons, K. (1999) N-glycans mediate the apical sorting of a GPI-anchored, raft-associated protein in Madin–Darby canine kidney cells. *J. Cell Biol.*, **146**, 313–320.
- Binden, C.I., Hale, G. and Waldmann, H. (1989) T8.4 synergistic complement-mediated cell lysis using pairs of antibodies. In Knapp, W., Dorken, B., Gilks, W.R., Rieber, E.P., Schmidt, R.E., Stein, H. and von dem Borne, A.E.G.K. (eds), *Leucocyte Typing IV*.

- White Cell Differentiation Antigens*. Oxford University Press, Oxford, UK, pp. 349–350.
- Bomsel, M., Prydz, K., Parton, R.G., Gruenberg, J. and Simons, K. (1989) Endocytosis in filter-grown Madin–Darby canine kidney cells. *J. Cell Biol.*, **109**, 3243–3258.
- Breitfeld, P.P., Casanova, J.E., Harris, J.M., Simister, N.E. and Mostov, K.E. (1989) Expression and analysis of the polymeric immunoglobulin receptor in Madin–Darby canine kidney cells using retroviral vectors. *Methods Cell Biol.*, **32**, 329–337.
- Brewer, C.B. and Roth, M.G. (1991) A single amino acid change in the cytoplasmic domain alters the polarized delivery of influenza virus hemagglutinin. *J. Cell Biol.*, **114**, 413–421.
- Brown, D.A. and London, E. (1998) Functions of lipid rafts in biological membranes. *Annu. Rev. Cell. Dev. Biol.*, **14**, 111–136.
- Chan, J.Y. et al. (2001) Relationship between novel isoforms, functionally important domains and subcellular distribution of CD164/endolyn. *J. Biol. Chem.*, **276**, 2139–2152.
- Chuang, J.Z. and Sung, C.H. (1998) The cytoplasmic tail of rhodopsin acts as a novel apical sorting signal in polarized MDCK cells. *J. Cell Biol.*, **142**, 1245–1256.
- Croze, E., Ivanov, I.E., Kreibich, G., Adesnik, M., Sabatini, D.D. and Rosenfeld, M.G. (1989) Endolyn-78, a membrane glycoprotein present in morphologically diverse components of the endosomal and lysosomal compartments: implications for lysosome biogenesis. *J. Cell Biol.*, **108**, 1597–1613.
- Garcia, M., Mirre, C., Quaroni, A., Reggio, H. and Le Bivic, A. (1993) GPI-anchored proteins associate to form microdomains during their intracellular transport in Caco-2 cells. *J. Cell Sci.*, **104**, 1281–1290.
- Gokay, K.E., Young, R.S. and Wilson, J.M. (2001) Cytoplasmic signals mediate apical early endosomal targeting of endotubin in MDCK cells. *Traffic*, **2**, 487–500.
- Gough, N.R., Zweifel, M.E., Martinez-Augustin, O., Aguilar, R.C., Bonifacio, J.S. and Fambrough, D.M. (1999) Utilization of the indirect lysosome targeting pathway by lysosome-associated membrane proteins (LAMPs) is influenced largely by the C-terminal residue of their GYXXΦ targeting signals. *J. Cell Sci.*, **112**, 4257–4269.
- Gut, A., Kappeler, F., Hyka, N., Balda, M.S., Hauri, H.P. and Matter, K. (1998) Carbohydrate-mediated Golgi to cell surface transport and apical targeting of membrane proteins. *EMBO J.*, **17**, 1919–1929.
- Harter, C. and Mellman, I. (1992) Transport of the lysosomal membrane glycoprotein lgp120 (lgp-A) to lysosomes does not require appearance on the plasma membrane. *J. Cell Biol.*, **117**, 311–325.
- Heilker, R., Spiess, M. and Crottet, P. (1999) Recognition of sorting signals by clathrin adaptors. *BioEssays*, **21**, 558–567.
- Henkel, J.R., Apodaca, G., Altschuler, Y., Hardy, S. and Weisz, O.A. (1998) Selective perturbation of apical membrane traffic by expression of influenza M2, an acid-activated ion channel, in polarized Madin–Darby canine kidney cells. *Mol. Biol. Cell*, **9**, 2477–2490.
- Höning, S. and Hunziker, W. (1995) Cytoplasmic determinants involved in direct lysosomal sorting, endocytosis and basolateral targeting of rat lgp120 (lamp-1) in MDCK cells. *J. Cell Biol.*, **128**, 321–332.
- Huet, G. et al. (1998) GalNAc- $\alpha$ -O-benzyl inhibits NeuAc $\alpha$ -3-glycosylation and blocks the intracellular transport of apical glycoproteins and mucus in differentiated HT-29 cells. *J. Cell Biol.*, **141**, 1311–1322.
- Hunziker, W. and Geuze, H.J. (1996) Intracellular trafficking of lysosomal membrane proteins. *BioEssays*, **18**, 379–389.
- Hunziker, W., Harter, C., Matter, K. and Mellman, I. (1991) Basolateral sorting in MDCK cells requires a distinct cytoplasmic domain determinant. *Cell*, **66**, 907–920.
- Ihrke, G., Martin, G.V., Shanks, M.R., Schrader, M., Schroer, T.A. and Hubbard, A.L. (1998) Apical plasma membrane proteins and endolyn-78 travel through a subapical compartment in polarized WIF-B hepatocytes. *J. Cell Biol.*, **141**, 115–133.
- Ihrke, G., Gray, S.R. and Luzio, J.P. (2000a) Endolyn is a mucin-like type I membrane protein targeted to lysosomes by its cytoplasmic tail. *Biochem. J.*, **345**, 287–296.
- Ihrke, G., Russell, M. and Luzio, J. (2000b) Endolyn contains lysosomal and apical targeting information in different domains of the protein. *Mol. Biol. Cell*, **11**, 205a.
- Ikonen, E. and Simons, K. (1998) Protein and lipid sorting from the *trans*-Golgi network to the plasma membrane in polarized cells. *Semin. Cell Dev. Biol.*, **9**, 503–509.
- Jacob, R., Preuss, U., Panzer, P., Alfalah, M., Quack, S., Roth, M.G., Naim, H. and Naim, H.Y. (1999) Hierarchy of sorting signals in chimeras of intestinal lactase–phlorizin hydrolase and the influenza virus hemagglutinin. *J. Biol. Chem.*, **274**, 8061–8067.
- Lipardi, C., Nitsch, L. and Zurzolo, C. (2000) Detergent-insoluble GPI-anchored proteins are apically sorted in Fischer rat thyroid cells, but interference with cholesterol or sphingolipids differentially affects detergent insolubility and apical sorting. *Mol. Biol. Cell*, **11**, 531–542.
- Martínez-Maza, R., Poyatos, I., López-Corcua, B., Núñez, E., Giménez, C., Zafra, F. and Aragón, C. (2001) The role of *N*-glycosylation in transport to the plasma membrane and sorting of the neuronal glycine transporter GLYT2. *J. Biol. Chem.*, **276**, 2168–2173.
- Migliaccio, G., Zurzolo, C., Nitsch, L., Obici, S., Lotti, L.V., Torrisi, M.R., Pascale, M.C., Leone, A. and Bonatti, S. (1990) Human CD8  $\alpha$  glycoprotein is expressed at the apical plasma membrane domain in permanently transformed MDCK II clones. *Eur. J. Cell Biol.*, **52**, 291–296.
- Mills, I.G., Jones, A.T. and Clague, M.J. (1998) Involvement of the endosomal autoantigen EEA1 in homotypic fusion of early endosomes. *Curr. Biol.*, **8**, 881–884.
- Mostov, K.E., Verges, M. and Altschuler, Y. (2000) Membrane traffic in polarized epithelial cells. *Curr. Opin. Cell Biol.*, **12**, 483–490.
- Nabi, I.R., Le Bivic, A., Fambrough, D. and Rodriguez-Boulán, E. (1991) An endogenous MDCK lysosomal membrane glycoprotein is targeted basolaterally before delivery to lysosomes. *J. Cell Biol.*, **115**, 1573–1584.
- Odorizzi, G. and Trowbridge, I.S. (1997) Structural requirements for basolateral sorting of the human transferrin receptor in the biosynthetic and endocytic pathways of Madin–Darby canine kidney cells. *J. Cell Biol.*, **137**, 1255–1264.
- Odorizzi, G., Cowles, C.R. and Emr, S.D. (1998) The AP-3 complex: a coat of many colours. *Trends Cell Biol.*, **8**, 282–288.
- Ohno, H., Aguilar, R.C., Yeh, D., Taura, D., Saito, T. and Bonifacio, J.S. (1998) The medium subunits of adaptor complexes recognize distinct but overlapping sets of tyrosine-based sorting signals. *J. Biol. Chem.*, **273**, 25915–25921.
- Owen, D.J. and Luzio, J.P. (2000) Structural insights into clathrin-mediated endocytosis. *Curr. Opin. Cell Biol.*, **12**, 467–474.
- Rodriguez-Boulán, E. and Gonzalez, A. (1999) Glycans in post-Golgi apical targeting: sorting signals or structural props? *Trends Cell Biol.*, **9**, 291–294.
- Röper, K., Corbeil, D. and Huttner, W.B. (2000) Retention of prominin in microvilli reveals distinct cholesterol-based lipid micro-domains in the apical plasma membrane. *Nature Cell Biol.*, **2**, 582–592.
- Scheiffele, P., Peranen, J. and Simons, K. (1995) *N*-glycans as apical sorting signals in epithelial cells. *Nature*, **378**, 96–98.
- Scheiffele, P., Roth, M.G. and Simons, K. (1997) Interaction of influenza virus haemagglutinin with sphingolipid–cholesterol membrane domains via its transmembrane domain. *EMBO J.*, **16**, 5501–5508.
- Ulloa, F., Franci, C. and Real, F.X. (2000) GalNAc- $\alpha$ -O-benzyl inhibits sialylation of *de novo* synthesized apical but not basolateral sialoglycoproteins and blocks lysosomal enzyme processing in a post-*trans*-Golgi network compartment. *J. Biol. Chem.*, **275**, 18785–18793.
- Weisz, O.A., Machamer, C.E. and Hubbard, A.L. (1992) Rat liver dipeptidylpeptidase IV contains competing apical and basolateral targeting information. *J. Biol. Chem.*, **267**, 22282–22288.
- Yeaman, C., Le Gall, A.H., Baldwin, A.N., Monlauzeur, L., Le Bivic, A. and Rodriguez-Boulán, E. (1997) The *O*-glycosylated stalk domain is required for apical sorting of neurotrophin receptors in polarized MDCK cells. *J. Cell Biol.*, **139**, 929–940.
- Zannettino, A.C., Buhning, H.J., Niutta, S., Watt, S.M., Benton, M.A. and Simmons, P.J. (1998) The sialomucin CD164 (MGC-24v) is an adhesive glycoprotein expressed by human hematopoietic progenitors and bone marrow stromal cells that serves as a potent negative regulator of hematopoiesis. *Blood*, **92**, 2613–2628.
- Zheng, X., Lu, D. and Sadler, J.E. (1999) Apical sorting of bovine enteropeptidase does not involve detergent-resistant association with sphingolipid–cholesterol rafts. *J. Biol. Chem.*, **274**, 1596–1605.

Received August 20, 2001; revised October 2, 2001;  
accepted October 3, 2001